Atmospheric Hygroscopic Ionogels with Dynamically Stable Cooling Interfaces Enable a Durable Thermoelectric Performance Enhancement

Feng Ni, Peng Xiao,* Chang Zhang, Wei Zhou, Depeng Liu, Shiao-Wei Kuo, and Tao Chen*

In thermoelectric generator (TEG) systems, heat dissipation from their cold sides is an accessible, low-cost, and effective way to increase the temperature gap for their thermoelectric performance enhancement. Although significant efforts have been dedicated mediated by hygroscopic hydrogel coolers as self-sustained alternatives for effective heat removal, it still remains a challenge for overcoming instabilities in their cooling process. The inevitable mechanical deformation of these conventional hydrogels induced by excessive water desorption may cause a detached cooling interface with the targeted substrates, leading to undesirable cooling failure. Herein, a self-sustained and durable evaporative cooling approach for TEG enabled by atmospheric hygroscopic ionogels (RIGs) with stable interfaces to efficiently improve its thermoelectric performance is proposed. Owing to its superior hygroscopicity, the RIGs can achieve higher heat dissipation for TEG through water evaporation than that of common commercial metal heat sinks. Moreover, its favorable adhesion enables the RIG closely interact with the TEG surface either in static or dynamic conditions for a durable thermoelectric performance enhancement. It is believed that such a self-sustained evaporative cooling strategy based on the RIG will have great implications for the enhancement of TEG's efficiency, demonstrating a great promise in intermittent thermal-energy utilizations.

1. Introduction

The world energy consumption has been on increasing trend of in recent decades, in which the generated heat is abundantly released, resulting in great amounts of energy waste, low working efficiency of installations, and heat pollution to the environment.[1,2] Thermoelectric technology from waste heat has provided a promising, efficient, and clean solution for energy recovery and power production.[3] In thermoelectric generator (TEG) working system, released heat can experience thermal diffusion between two sides to accumulate on its cold side, thereby leading to ever-reduced temperature differences (ΔT) for prominent degeneration of thermoelectric performance.[4,5] Compared with the endeavor of promoting inherent thermoelectric figure of merit (ZT) of TEG, the direct cooling strategy can enlarge the ΔT and simultaneously boost their electric output in an efficient, low-cost and accessible way.[6–8] Currently, cooling strategies for the TEG have active cooling and passive cooling. For the active approaches, the TEG demonstrates a high heat dissipation, but heavily relies on extra energy supply and cumbersome engineering design, limiting their applications in large-scale or portable scenes.[6] Whereas, passive cooling strategies, such as metal heat sinks, radiative cooling and materials phase change, have been developed to provide alternative solutions to remove heat from TEG surface without carbon footprints.[7,8] Specifically, among these passive strategies, due to the high latent heat of water (≈ 2450 J g^{-1}), water evaporation is considered as a promising alternative to dissipate heat, but requires continuous water supply and extra energy consumption.[9] Generally, the atmosphere contains huge amounts of moisture resource existed in vapor form, which enables sustainable and ubiquitous water supply.[10–15] Therefore, exploiting renewable atmospheric water resources for a self-sustained evaporative cooling strategy is actively requested for efficient heat dissipation. Recently, diverse hygroscopic hydrogel materials have been reported to achieve effective and longer evaporative cooling due to its high-capacity moisture sorption.[16–18] However, when long-term cooling is conducted, these conventional

F. Ni, P. Xiao, C. Zhang, W. Zhou, D. Liu, T. Chen
Key Laboratory of Marine Materials and Related Technologies
Zhejiang Key Laboratory of Marine Materials and Protective Technologies
Ningbo Institute of Materials Technology and Engineering
Chinese Academy of Sciences
Ningbo 315201, China
E-mail: xiaopeng@nimte.ac.cn; tao.chen@nimte.ac.cn
F. Ni, P. Xiao, C. Zhang, W. Zhou, D. Liu, T. Chen
School of Chemical Sciences
University of Chinese Academy of Sciences
Beijing 100049, China
S.-W. Kuo
Department of Material and Optoelectronic Science
Center of Crystal Research
National Sun Yat-Sen University
Kaohsiung 804, Taiwan

**ADVANCED
SCIENCE NEWS**

www.advancedsciencenews.com

**ADVANCED
MATERIALS**

www.advmat.de
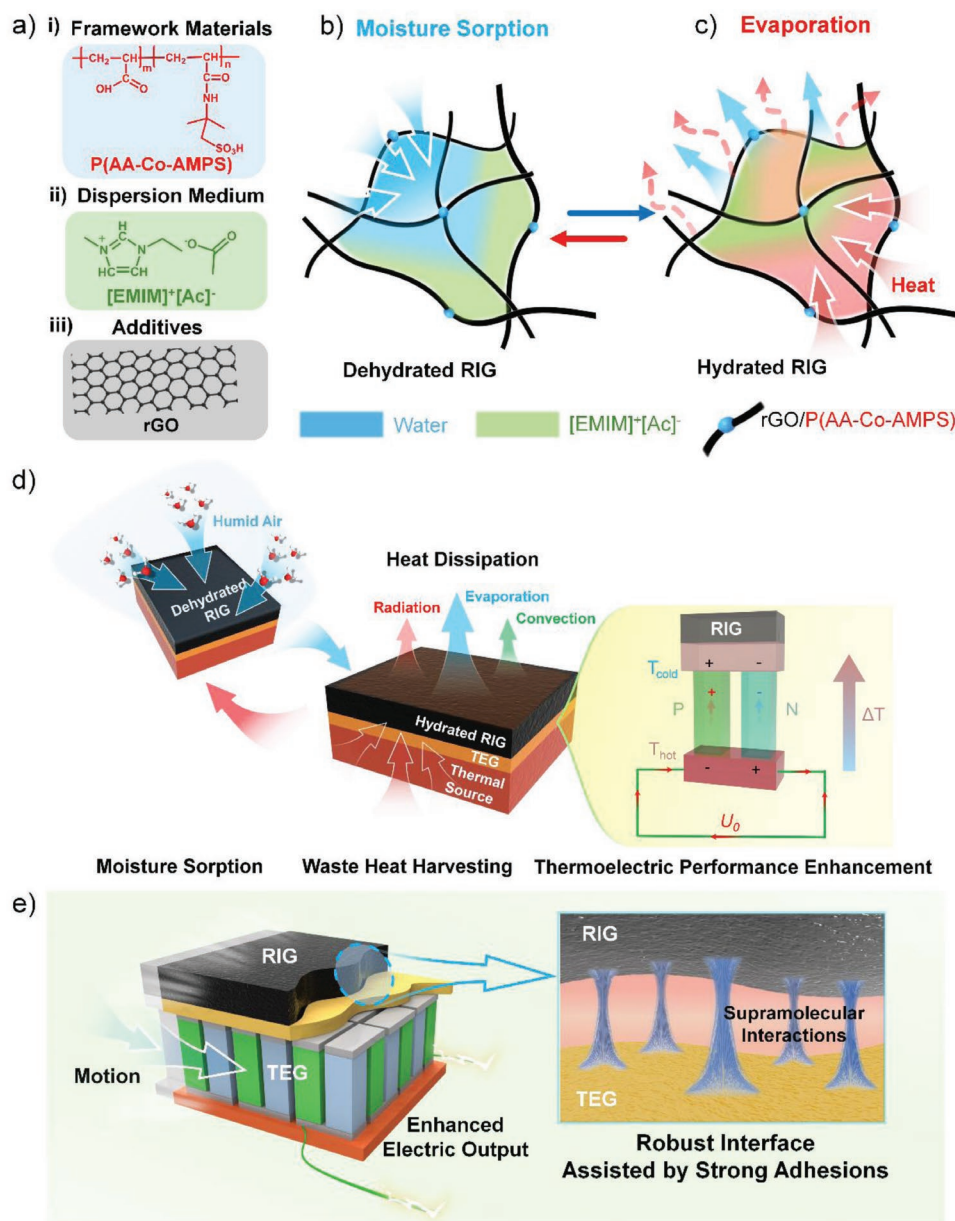
Scheme 1. Schematics of atmospheric hygroscopic RIG with a dynamically stable cooling interface for durable thermoelectric performance promotions. a) Components composited of RIG and their structures. b,c) The evaporative-cooling working principle of RIG for heat dissipation, b) moisture sorption from the air with the dehydrated RIG, and c) water evaporation from the hydrated RIG induced by thermal energy could dissipate heat. d) The hygroscopic RIG was employed to cool down TEG cold side to expand ΔT for efficient thermoelectric performance enhancement though moisture sorption and desorption. e) Since its strong adhesions, the RIG could achieve a durable evaporative cooling with a robust contact interface with the TEG both in static and moving states to boost its thermoelectric performance.

hydrogels may experience excessive water desorption and further result in severely mechanical deformation, causing their cooling performance decline and even failure.[17,19] In addition, due to their weak adhesive interfaces, these reported hydrogels present poor adaptability either in portable or moving occasions, which may be a risk of detaching from the cooling interface. Therefore, it still remains a challenge for developing a high-efficient evaporative cooling technology characterized with a stable cooling interface both in static and dynamic conditions.

Herein, we demonstrated an atmospheric hygroscopic ionogel with a stable cooling interface for efficient and durable thermoelectric performance enhancement of the TEG through atmospheric moisture sorption and evaporation. As shown in **Scheme 1**a, a hydrophilic poly (acrylic acid-*co*-2-acrylamido-2-methylpropane sulfonic acid) (P(AA-*co*-AMPSA)) network was selected to accommodate hygroscopic liquid of 1-ethyl-3-methyl-imidazolium acetate ([EMIM][Ac]) and reduced graphene oxide (rGO) additives to obtain a solid rGO/ionogel (RIG), where rGO was introduced to improve its IR emittance and thermal

conduction for enhanced heat dissipation (Figures S1–S3, Supporting Information). The working principle of the proposed RIG for evaporative cooling was illustrated in Scheme 1b,c. Since its intense hygroscopicity, the dehydrated RIG was able to spontaneously capture moisture from the atmosphere. When the hydrated RIG received thermal energy, the absorbing water would be evaporated, accompanying with a great amount of heat migration from the targeted heated surface. As a proof-of-concept, we employed this RIG as a self-sustained cooler applied to TEG cold side though moisture sorption and desorption, aiming to elevate the ΔT across the TEG device to efficiently boost its conversion of waste heat into electricity (Scheme 1d). Moreover, benefiting from the addition of [EMIM][Ac], the resulted RIG demonstrated strong adhesions mediated by multiple supramolecular forces, allowing a stable contact interface with TEG for durable performance enhancement of TEG either in a static state or in the motion (Scheme 1e). We convince that such a hygroscopic RIG with strong adhesive properties can inform further developments of evaporative coolers targeting at practical requirements of heat dissipation for the TEG.

2. Results and Discussion

2.1. Hygroscopic Mechanisms and Performances of RIG

At present, various prototypes using porous hygroscopic materials (e.g., metal–organic frameworks (MOFs)[20–23] and hygroscopic-inorganic-salt doped aerogel materials[11,19,24–26]) have been exploited to capture moisture from environment. However, these reported porous hygroscopic materials generally showed relatively low sorption amount of moisture due to the limited pore volumes and poor diffusion factors.[18,27] By contrast, well-designed hydrophilic polymeric networks combined with hygroscopic liquid medium can be potential alternatives for sustainable and high-capacity moisture sorption.[28] As such, we have designed a hygroscopic RIG with preferable moisture sorption to achieve a self-sustained passive evaporative cooling for the TEGs. Typically, the high affinity of sorbents surface to water molecules facilitates moisture trapping from the air.[15] In order to analyze chemical functional groups on the RIG surface, the attenuated total reflection-Fourier transform infrared spectroscopy (ATR-FTIR) was adopted (**Figure 1**a). The results showed that there was a characteristic peak at ≈647 cm^{-1} of S—O stretching of sulfonate groups.[29] Moreover, the peaks located at ≈619 and 1167 cm^{-1} stemmed from the out-plane bending vibration of the C—H bond and the C—N stretching vibration, respectively, which belonged to the charged imidazole ring of [EMIM][Ac].[10] Furthermore, the peaks at ≈1388 and 1558 cm^{-1} were corresponded to symmetric and asymmetric stretching of COO$^-$ groups.[24] As a result, these strongly polar groups appearing on the surface of the dehydrated RIG can endow it an excellent hygroscopicity through the formation of hydrogen bonds or electrostatic interactions with water molecules. In comparison with the dehydrated RIG, the sample in a humid environment of 90% RH for 12 h demonstrated a higher and wider peak at 3359 cm^{-1}, which derived from stretching vibrations of —OH groups of water molecules. The result indicated

that there was a remarkable hygroscopic process on the RIG surface.[30] In addition, the liquid [EMIM][Ac] inside RIG can provide an osmotic pressure to drive water migrations from its surface to interior as our previously reported.[28] The ionic liquid can reactivate sorption sites on the surface, and thus ensure a sustainable moisture capture. As a result, the RIG demonstrated a rapid and high-capacity water uptake of 0.96, 0.50, and 0.24 g g^{-1} for 12 h at 90%, 70%, and 50% RH, respectively (Figure 1b). Note that the hydrated RIG represented a desirable chemical stability and could further maintain its hygroscopicity when experienced thermal redehydration, which was highly demanded by self-sustained evaporative cooling (Figure S4a,b, Supporting Information). Moreover, moisture sorption isotherms of RIG were also measured to assess its capability of water uptake under different temperatures (Figure 1c). In our experiment, the RIG performed similar sorption behaviors from 15 to 35 °C, in which its equilibrium values of water uptake were 1.41, 1.25, and 0.96 g g^{-1} at 90% RH and the temperature of 15, 25, and 35 °C, respectively. These results indicated the RIG possessed competitive hygroscopic capacities with other reported start-of-art sorbent materials.[10,12,18,25,31]

In order to further characterize the structural stability of RIG after moisture sorption, the hydrated sample was measured by rheological tests (Figure 1d). Although there was a decrease of storage modulus, the hydrated RIG still demonstrated an elastic behavior similar to the original dehydrated state. Moreover, storage and loss modulus of the RIG can both restore to the initial values when its absorbed water was re-evaporated (Figure S4c, Supporting Information). Such a stable cross-linked structure enabled the RIG meet requirements for moisture sorption and evaporative cooling. Additionally, thermogravimetric analysis (TGA) was conducted to measure the decomposition temperature of RIG samples. As shown in Figure 1e, apart from the initial water desorption, the hydrated RIG displayed a similar thermal decomposition behavior as the dehydrated RIG, at the high temperature. The decomposition temperature of the hydrated RIG could reach up to ≈210 °C, at which its inner [EMIM][Ac] begun to volatilize (Figure S5, Supporting Information). These results illustrated a desirable thermal stability of material for the RIG, and also indicated that the RIG could adapt to a broad operation temperature for evaporative cooling. Moreover, for the evaporation cooling, the thermal stability of RIG's cross-linked structure was further considered. When surrounding temperature arose from 25 to 120 °C, the storage modulus of RIG always showed a higher value than that of its loss modulus, and the value of corresponding tanθ also retained less than 1.0 (Figure 1f). It means that RIG is capable of maintaining stable solid and elastic structure and cannot be destroyed in aforementioned temperature ranges typically used for evaporative cooling.[32] Hence, the hydrated RIG can achieve a water desorption in such a wide temperature region as described above. As a result, the RIG samples hydrated in 90% RH for 12 h were able to achieve efficiently water desorption in the environments of 60 to 90 °C. Notably, all absorbed water of the hydrated RIG can be fully released within 2 h at 90 °C with a fast desorption kinetics (Figure 1g). Furthermore, from the perspective of practical operation, the cyclic sorption stability of the RIG should be considered. As shown in Figure 1h, the RIG demonstrated a repeated hygroscopic capability without obvious

**ADVANCED
SCIENCE NEWS**

www.advancedsciencenews.com

**ADVANCED
MATERIALS**

www.advmat.de
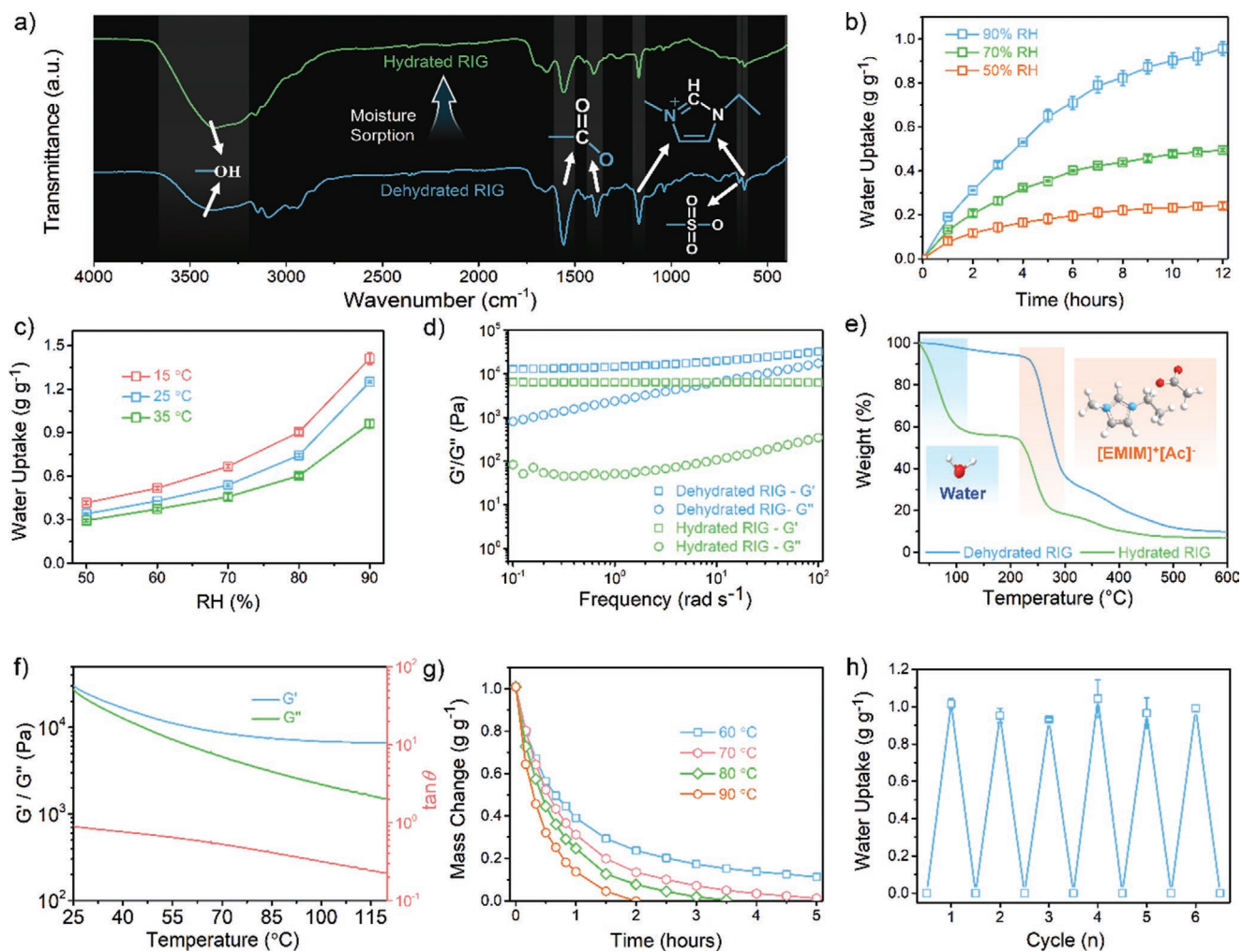
Figure 1. Assessments of moisture sorption and desorption of RIG. a) ATR-FTIR spectra of the RIG surface before and after moisture sorption. b) The moisture-sorption kinetics of RIG at 25 °C, and in various relative humidity (RH) from 50% to 90% for 12 h. c) Moisture-sorption isotherms of RIG at 15, 25, and 35 °C, respectively. d) Rheological properties of the dehydrated RIG and the hydrated RIG, where the hydrated RIG was obtained from the dehydrated RIG through a moisture sorption at 90% RH for 12 h. e) TGA curves of RIG from 25 to 600 °C, and the insets are the chemical structures of water and [EMIM][Ac], respectively. f) The stability characterization of cross-linked networks of RIG though temperature-related rheological tests. g) Water desorption curves of the hydrated RIG (treated in 90% RH for 12 h) in the environments of different temperatures, varying from 60 to 90 °C. h) Cyclic performances of moisture sorption–desorption of RIG, in which sorption conditions are 25 °C and 90% RH, and desorption ones are 90 °C and 10% RH, respectively.

decline, where the average sorption amount was ≈0.98 g g^{-1} within six cycles. Such a structure-stable RIG with large sorption amounts, fast sorption–desorption kinetics, and repeatable hygroscopic behaviors was suitable for evaporative cooling on TEG systems to promote their electric generation in occasions harvesting low-temperature waste heat.

2.2. Evaporative Cooling of RIG for Thermoelectric Performance Enhancement

To evaluate evaporative cooling of the RIG, a commercial TEG system was employed to validate its feasibility. The detailed experiment setups and processes were schematically displayed in Figure S6 (Supporting Information), where the RIG was directly placed on the TEG cold side for self-sustained

evaporative cooling. In the practical operation, the RIG can experience an intermittent working principle: 1) the dehydrated RIG first spontaneously absorbs moisture from surroundings and stores it inside when the TEG is in dormancy; Afterward, 2) the hydrated RIG dissipates heat from the TEG through three ways, including water evaporation, thermal convection, and thermal radiation, to improve its thermoelectric performance. In this process, the moisture sorption amount of the RIG is closely related to eventual cooling effect for the TEG, and thus requires to be further measured. Accordingly, abovementioned setups were exposed to humid environments of 25 °C to characterize moisture sorption of the RIGs. Benefited from their excellent hygroscopicity and intrinsic swellable property, these resultant RIG samples achieved rapid and high-capacity moisture uptakes of 0.59, 0.28, 0.14 g cm^{-2} at 90%, 70%, and 50% RH, respectively, within 12 h (Figures S7 and S8, Supporting
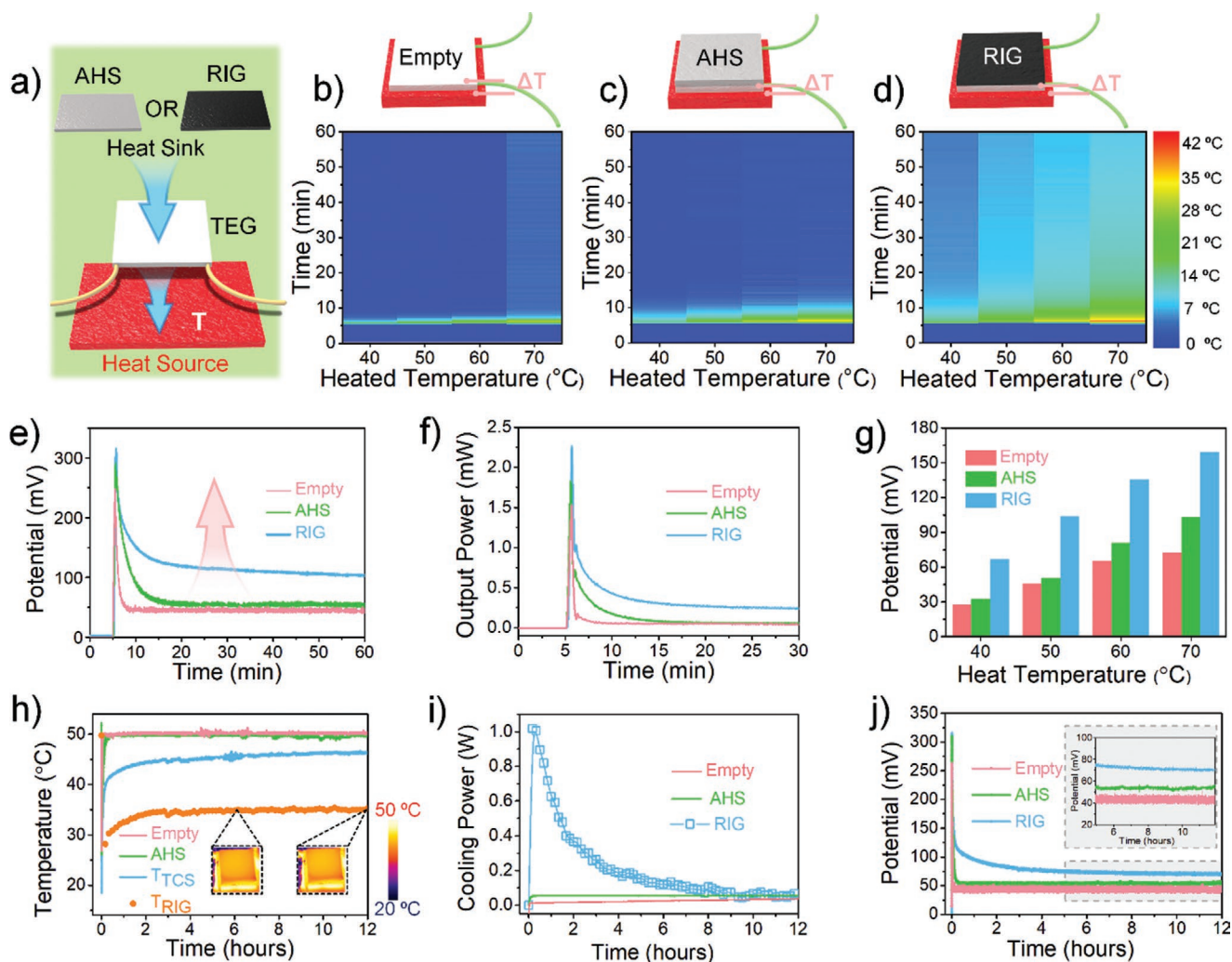
Figure 2. Evaporative cooling of hygroscopic RIG for thermoelectric performance promotion. a) Schematic of cooling setups for TEG system, in which T (heat source temperature) refers to the temperature of the TEG hot side. b–d) ΔT across the TEG device with different cooling systems as a function of time and heat source temperatures, in which TEG was in dormancy in the first 5 min. b) TEG without heat sink (Empty), c) TEG with commercial Al heat sink (AHS), d) TEG with hydrated RIG that pre-treated in 90% RH for 12 h (RIG). e) The generated voltages of TEG with different cooling systems at the heat source temperature of 50 °C. f) The output powers of TEG with three cooling modes at the heat source temperature of 50 °C. The results indicated that RIG was capacity of efficiently and sustainably improve the electric generation of TEG, comparing with AHS and Empty modes. g) A comparative chart of the generated voltage of TEG with different cooling system at different heat source temperatures. h) The varieties of temperatures against as time at the heat source temperature of 50 °C for 12 h. The inserts were IR images of RIG after 6 and 12 h, respectively. i) The cooling powers of TEGs, and j) the corresponding generated voltages with different cooling systems in Figure 3h, and the inset was the enlarged view of the gray area.

Information). Notably, these actual moisture sorption amounts of RIG were superior to most of reported evaporative-cooling systems in a wide range of humidity,[9,16,17,19,33,34] thus showing a great promise in evaporative cooling (Table S1, Supporting Information). In addition, desorption rates of absorbed water are crucial factors for heat removal, which mainly depended on heat source temperatures. In our experiments, the TEG was selected to harvest low-grade heat, and thus its heat source temperatures were accordingly set from 40 to 70 °C. As shown in Figure S9 (Supporting Information), it is observed that various RIG samples hydrated in 50% to 90% RH all experienced a huge water desorption when the heat source temperature was 50 °C, in which their water desorption amounts were as high as 0.07, 0.16, and 0.34 g cm^{-2}, respectively. Moreover, the

absorbed water by the RIG can also be apparently evaporated even at a lower temperature of 40 °C (Figure S10, Supporting Information). These discussed results illustrated that the RIG was capable of realizing effective heat migrations under these low-temperature working conditions of the TEG.

In order to highlight the superiority of our RIG on cooling for TEG, we selected the TEG systems with commercial Al heat sink (marked as AHS) and without any heat sink (marked as Empty) for comparisons, and ΔT across the TEG device was extracted to represent their cooling effects (**Figure 2**a–d; and Figure S11, Supporting Information). The results showed that the AHS exhibited a powerful heat dissipation just at the early stage owing to its excellent thermal conduction, but quickly had a thermal-induced cooling invalidation after ≈5 min

**ADVANCED
SCIENCE NEWS**
www.advancedsciencenews.com

**ADVANCED
MATERIALS**
www.advmat.de

(Figure 2b). By contrast, the hydrated RIG indicated a stronger and more sustainable cooling capacity for the cold side of running TEGs. Since water evaporation took away large amounts of heat, the ΔT of the TEG with RIG performed higher value than that of other two systems for selected heat source temperatures (Figure 2c). Meanwhile, ΔT of the TEG with RIG was also related to its corresponding heat source temperature, which demonstrated an increasing trend with the rise of the heat source temperature. This result might derive from faster water evaporated rates of hydrated RIG under high heat source temperatures (Figure 2d; and Figure S10, Supporting Information). Note that this improved cooling performance on the TEG cold side can eventually lead to an enhanced power generation of the TEG. As shown in Figure 2e, the TEG with RIG always presented the highest generated voltage among above three cooling systems, which was double than that of AHS mode (60 mV) and three times than that of Empty mode (40 mV) at the working equilibrium state when the heat source temperature of the TEG was 50 °C. The output power of TEG at the heat source temperature of 50 °C was displayed in Figure 2f. Compared with Empty mode, the maximum power of TEG with RIG was prominently promoted from 0.05 to 0.25 mW at the equilibrium working stages. Such a five-times enhancements of TEG performance enabled by evaporative cooling of RIG was more facile and feasible than conventional methods through improving inherent materials factors of TEG. As larger ΔT can be induced by a higher heat source temperature, the TEG thus demonstrates a stronger electric output. As expected, the equilibrized voltage of the TEG equipped with hydrated RIG also showed an increasing trend with its heat source temperature improving (Figure S12, Supporting Information). After heating for 55 min, the resulted TEG systems can still maintain output potentials of 160, 140, 100, and 70 mV at the heat source temperatures of 70, 60, 50, and 40 °C, respectively. In these cases, there were all significant improvements on electricity-generation performance of the TEG with RIG comparing to ones with another two cooling modes (Figure 2g).

To investigate the effective cooling duration of the RIG on TEG, we conducted a long-term comparative experiment (12 h). The relevant setups were illustrated in Figure S13 (Supporting Information), where Infrared (IR) camera was chosen to record the temperature of RIG (T_{RIG}) and the thermal couples were attached to detect the cold-side temperature of TEG (T_{TCS}). Prior to cooling for TEG, the hydrated RIG sample was put in a 90% RH environment to absorb moisture for 12 h. As a representative, the heat source temperature of the TEG was set as 50 °C. Even after working for 12 h, the ΔT across the TEG could still maintain 3.7 °C through attaching a hydrated RIG on the TEG, which was far higher and more sustainable than that of the TEG coupled with commercial AHS (Figure 2h). Also, as shown in the insert of Figure 2h, the resulted RIG could quickly dissipate heat to the surroundings due to its high thermal emissivity, thus the ΔT between RIG and TEG hot side was always about 15 °C. Different from limited and tiny cooling effect of commercial AHS, the hydrated RIG can provide an enormous heat dissipation power for TEG to promote its electric generation for a longer period. Moreover, the corresponding cooling power of RIG was calculated by energy balance model (Figure S14, Supporting Information). The results indicate that RIG can retain a

significant cooling behavior during the whole 12 h, and its maximum transient cooling power can reach up to 1.0 W, which is competitive with recently reported work based on hygroscopic MOFs[9] (Figure 2i). Similarly, the electric output of TEG with RIG was also higher than that of TEG systems with AHS or Empty modes, which was shown in Figure 2j. Furthermore, the strengthened cooling time that was defined as the moment of cooling power closed to that of the TEG with commercial AWH, was able to sustain at least 12 h. The working time was expected to satisfy the requirements of long-term operation of TEG (inset of Figure 2j). More importantly, the cooling effects of the RIG for the TEG can be fully regenerated due to its considerable hygroscopicity. Even after a long time, the TEG still maintained an effective cooling for the TEGs as before (Figure S15, Supporting Information). Therefore, such a self-sustained RIG with long lifetime shows diverse potentials in some intermittent applications of solar-thermal-thermoelectric generators, industrial-waste-heat harvesting (e.g., transformer box, mobile base station, etc.).

Notably, the cooling performance of the RIG for the TEG would be also affected by the environmental humidity. Owing to suppressed water evaporation at high RHs, the RIG has a slight cooling performance decrease for TEG with the increase of the RH (Figure S16, Supporting Information). Moreover, the RIG also demonstrated great potentials in further improving its cooling performance though the design of three-dimensions structures. As shown in Figure S17 (Supporting Information), a fin-type RIG (F-RIG) achieved a more considerable heat dissipation from the TEG than that of normal plate-type RIG (P-RIG). It enabled the TEG a more higher output voltage for 12 h under the same conditions.

In addition, we carried out an on-site experiment to explore potential functions of the electric output enhancement of TEG. The electric circuit diagram and physical setups were shown in Figure S18a,b (Supporting Information). In our system, a heater was used to simulate the hot surface of a running machine to supply waste heat, and a potential booster was applied to enlarge the resulted output voltage of TEG, which aimed to light up a thermo/hygrometer with an operation voltage of 3 V. As displayed in Figure S18c (Supporting Information), the output voltage of the TEG with hydrated RIG could always maintain more than 3 V within 12 h, yet that of TEG with AHS only lasted for 9 min when the heat source temperature was 60 °C. Eventually, the thermo/hygrometer can be lighted up for at least 12 h by the TEG with RIG. In contrast, the TEG with AHS only lasted for 9 min (Figure S18d, Supporting Information). In this content, this evaporative cooling strategy based on RIG can realize a significant and sustainable enhancement on thermoelectric performance of TEG, which was promising to power for high-operation-voltage electronics.

2.3. Dynamically Stable Cooling Interfaces of RIG Assisted by Strong Adhesions

A robust and stable adhesive interface between the TEG and the heat sink was essential to achieve heat dissipation, and thus required to be considered. Owing to their superb moisture sorption, some hygroscopic polymer hydrogels have been

developed for evaporative cooling.[16,17] In this process, these hydrogel coolers can attach on the static adherends owing to their low mechanical modulus and limited adhesive forces. However, inevitable mechanical deformations (e.g., bending and shrinkage) of these conventional hydrogels during the water desorption process would cause a poor contact with the TEG surface,[17,19] leading to a rapid cooling performance deterioration. Moreover, these solutions might not be suitable for continuous heat removal, particularly, in moving occasions. Thus, a stable and robust cooling interface either in static or dynamic cooling condition is actively requested. According to the interface stability model proposed by Roger et al.,[35–37] improving interfacial adhesion is one of effective approaches for coolers to maintain a stable interfacial contact with the TEG surface. In this regard, our RIG was regarded as a desirable candidate for gel-based coolers to create a robust interface with the targeted substrates due to its strong adhesive features.

The superior adhesions of the RIG were ascribed to the synergy of its chemical bonding, topology of connection, and energy dissipation, in which the chemical bonding derived from the specific functional groups of the polymeric network and ionic liquids dominated the adhesive process. Owing to the introduction of [EMIM][Ac], the RIG demonstrated a large amount of exposed bondable sites on its surface. It can bond with different adherends through diverse supramolecular interactions, including hydrogen bonds, electrostatic, ion-dipole, coordination, and hydrophobic interactions[38–41] (**Figure 3**a). In detail, for the hydrophilic substrates surface, the hydrogen bonds, electrostatic, and coordination may account for the stable interaction. Whereas, ion-dipole and hydrophobic interactions were responsible for the hydrophobic substrates, such as fluorinated surface. When the RIG was pressed onto the adherends, it fully conformed to the adherend surface to enhance its adhesions.[42,43] Moreover, the reversible ion–ion interactions between polymeric networks and ILs in the RIG also provided a dissipation mechanism, leading to an extra energy for the interfacial crack propagation.[38,44,45] As a result, the RIG performed considerable adhesive properties for various substrates, such as TEG, glass, metal (Al), PET, and PTFE. As shown in Figure 3b, RIG strips with sizes of $10 \times 10 \times 5$ mm³
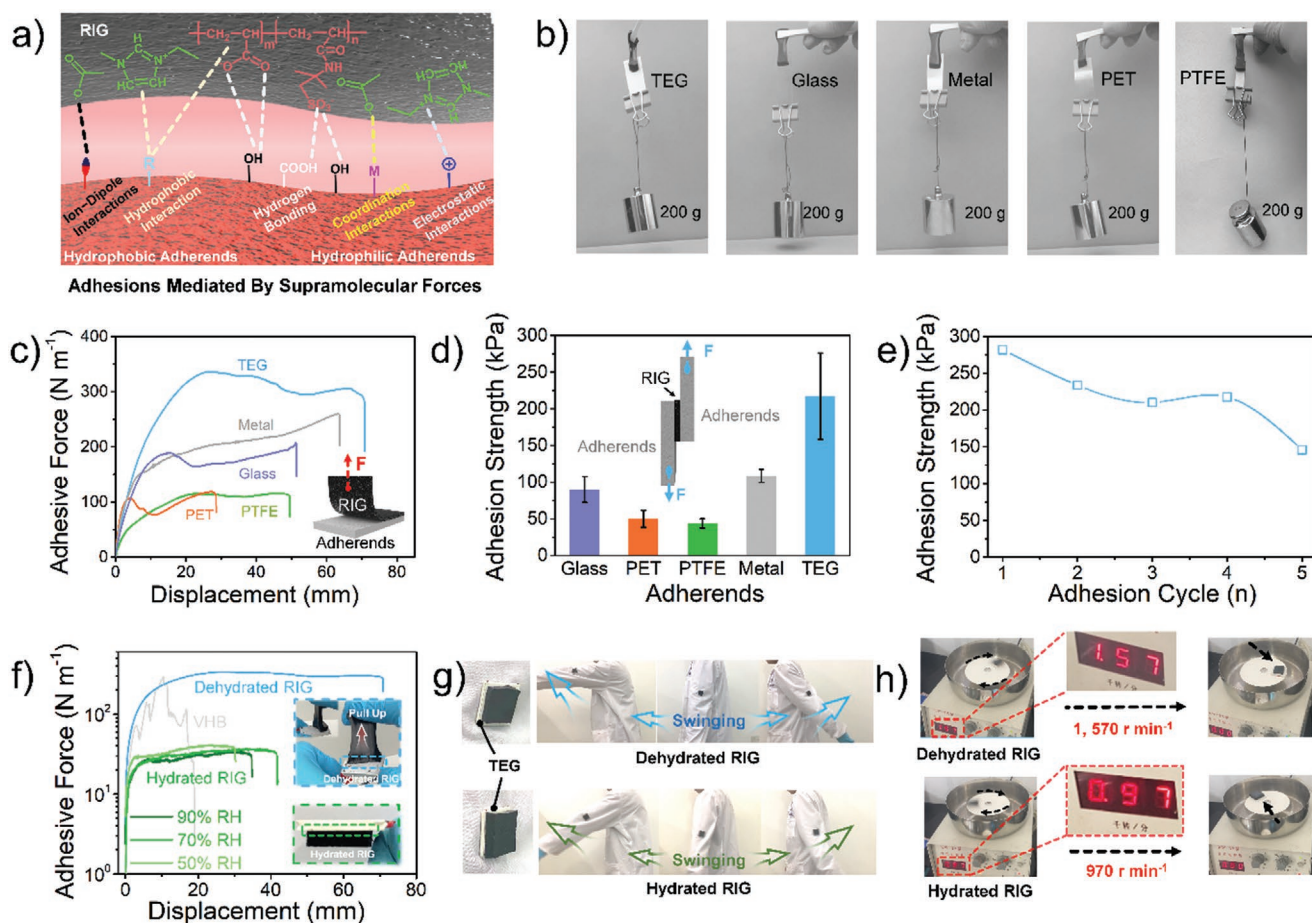
Figure 3. The strong adhesions and robust adhesive interfaces of RIG in dynamic conditions. a) The adhesive mechanisms between RIG and adherends. b) RIG can bear 200 g of weight attaching on various adherends with an adhesive area of 10×10 mm. c) Interfacial adhesive forces per length between RIG and different adherends, measuring by standard 90° peel tests. d) Lap sheer tests of RIG with various adherends. e) Cyclic adhesion of RIG on the TEG surface. f) Interfacial adhesive forces per length of dehydrated and hydrated RIGs on TEG surface, in which the hydrated ones were pre-processed in different RHs for 12 h. The gray curve was the adhesive forces between the commercial VHB and the TEG surface. The inserts were physical photos of dehydrated RIG and hydrated RIG after a moisture sorption in 90% RH for 12 h. g) The adhesive stabilities of dehydrated and hydrated RIG on a drastically swinging arm. h) The adhesive stabilities of dehydrated and hydrated RIG on the high-speed rotating plate.

can tightly stick to above adherends to lift up an object of 200 g (Movie S1, Supporting Information). Furthermore, 90° peeling-off and lap sheer measurements were conducted to assess the adhesive force between resulted RIG and various substrates. The adhesive forces per samples width was plotted against the displacement in Figure 3c. Owing to its hydrophilic feature and coarse structure (Figure S19, Supporting Information), the TEG surface demonstrated a superhigh adhesive forces reaching up to 323 N m^{-1} with the resulted RIG, which was even superior to recently reported adhesive polymer gels.[46,47] In lap sheer tests, the RIG all showed high adhesive strengths for various adherends, which reached to 89.98, 49.95, 43.77, 108.61, 217.2 kPa to glass, PET, PTFE, metal (Al) and TEG surface, respectively (Figure 3d). As displayed in Figure 3e, the RIG still maintained intense adhesive forces to TEG surface after five times lap sheer tests, ensuring the capability of its cyclic usages. Moreover, the adhesive behavior of RIG after moisture sorption was also evaluated. Owing to the synergy effect of their decreased modulus and rapid transformation of interfacial water, the RIG also demonstrated an intense adhesion with the targeted TEG surface after considerable moisture sorption[43,48,49] (Figure S20, Supporting Information). As shown in Figure 3f, hydrated RIG samples after absorbing moisture in different RHs for 12 h presented comparable interfacial adhesive forces, reaching to 34.03, 36.87, and 40.17 N m^{-1} at the RH of 90%, 70%, and 50%, respectively. Although there was an obvious decrease of adhesive forces after moisture, the hydrated RIG still demonstrated a competitive adhesion with reported adhesive wearable hydrogels,[43,46,50] and was capable of tightly attaching itself on the TEG surface (inset of Figure 3f). Apart from static adhesions, the adhesive stability between resulted RIG and TEG surface in some moving scenarios was also considered. Targeting at applications of wearable TEG, RIG samples equipped on the TEG were measured on a swinging arm. As expected, both resulted RIG samples can closely adhere onto the TEG surface even exposed to a vigorous swinging condition (Figure 3g; and Movies 2–3, Supporting Information). Furthermore, a high-speed rotating plate was selected to imitate a fast-moving application interface. As illustrated in Figure 3h, the dehydrated and hydrated RIGs were able to endure 1570 and 970 r min^{-1} rotation, respectively (Movie 4, Supporting Information). These results indicate that the proposed RIG can keep a robust and intense adhesion on TEG surface before and after moisture sorption, which is beneficial to achieve stable evaporative cooling for the TEG both in static and dynamic conditions.

In addition to adhesive strength, structural change derived from water desorption for hygroscopic polymeric gels during evaporative cooling should be premeditated, which might cause a detached behavior at their contact interfaces with targeted adherends. For comparison, a RHG sample that had weak adhesive forces with TEG surface was selected to dissipate excessive heat from TEG surface. As shown in **Figure 4**a, a severe warpage of RHG occurred within only 30 min, which was unfavorable for continuous cooling (Movie 5, Supporting Information). Prominently, the hydrated RIG can invariably maintain stable attachment on the TEG surface during a 12 h evaporative cooling (Figure 4b). To further explore the potential reasons, we conducted finite element simulations by COMSOL

software. From the results we can find that the strong adhesions between RIG and TEG surface can remarkably alter the stress distribution during water evaporation (Figure 4c,d). When its bottom was unconstrained with remarkably weakened or even disappeared adhesion forces, RHG could yield a series of stress concentrations around itself, attributed to asymmetric water evaporation. These stress concentrations eventually caused a prominent deformation of RHG, which was subsequently detached from the TEG surface (Figure 4c; and Figure S21, Supporting Information). However, the stress concentrations of RIG would just distribute in its four corners under the constraint of its intense adhesion (Figure 4d; and Figure S22, Supporting Information). Under the synergetic interactions of the increasing adhesion forces of RIG during the dehydration process, RIG can always tightly attach onto the TEG surface. Besides, the RIG with a strong adhesive interface is expected to actively adapt to dynamically moving surface for stable evaporative cooling of TEG, which can endure the external force generated by the motions and maintain a closed adhesion with the TEG (Figure 4e).

To verify this feasibility, we built up the TEG system with RIG on an industrial engine. The working engine can generate a lot of waste heat, and its surface temperature could rapidly reach up to ≈103 °C within 300 s (Figure 4f). In addition, this engine produced a huge oscillating vibration with the acceleration of ≈63.8 m s^{-2} (Figure 4g). As demonstrated in Figure 4h, the RHG without intense adhesions finally detached from TEG surface, which was jointly caused by its warpage and forces induced by oscillation of working engine. Meanwhile, strongly adhesive RIG was able to maintain stable attachments on the TEG and simultaneously achieved an effective evaporative cooling for TEG during engine working (Movie 6, Supporting Information). Furthermore, the corresponding output voltage of TEG was measured in Figure 4i. Owing to the detachment, the TEG with RHG showed a deteriorating cooling performance on a running engine similar to TEG without cooling system. By contrast, there was an effective improvement on the electric generation of the TEG with RIG during the whole testing, indicating that RIG indeed remained a stable evaporative cooling interface even on a running engine with huge vibrations.

3. Conclusion

In summary, we demonstrated a hygroscopic ionogel (RIG) for efficient and stable evaporative cooling for TEG to durably boost its thermoelectric performances. The hydrophilic polymeric cross-linked networks of P(AA-co-AMPSA) can accommodate hygroscopic [EMIM][Ac] liquid and functional rGO additives inside itself to form a hygroscopic RIG, demonstrating a capability of rapid, high-capacity, and repeatable moisture sorption. The resulted RIG can realize an unprecedented moisture uptake of 0.96 g g^{-1} for 12 h at 25 °C and 90% RH, which is competitive to reported hygroscopic materials. As such, the hydrated RIG exhibited an impressive evaporative cooling for the TEG to prominently enhanced its thermoelectric generation. Compared to commercial Al heat sink, there is a two-times enhancements on the output performance value of the TEG

**ADVANCED
SCIENCE NEWS**

www.advancedsciencenews.com

**ADVANCED
MATERIALS**

www.advmat.de
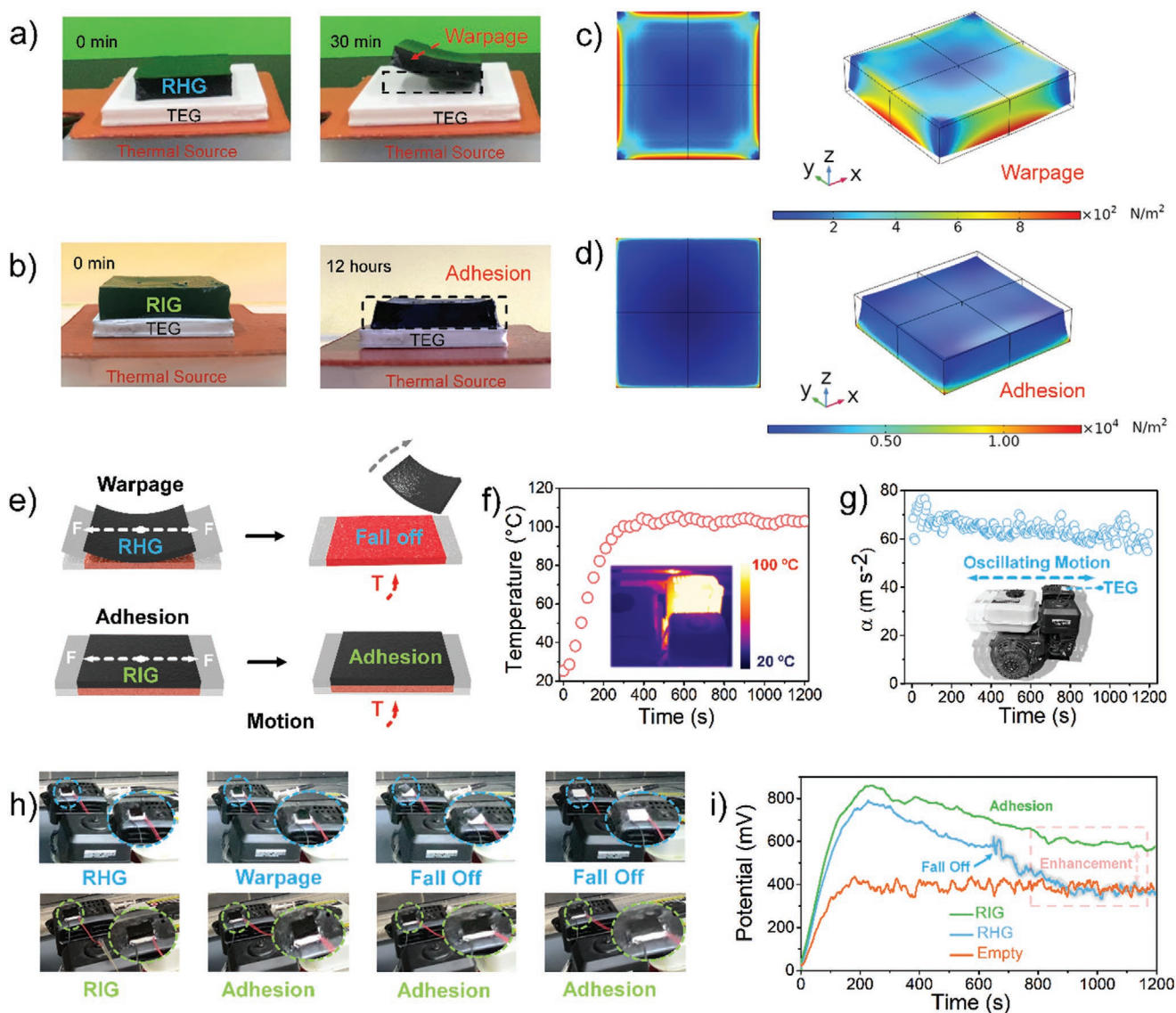
Figure 4. The dynamically stable cooling interface of RIG for a durable thermoelectric performance promotion. a) A RHG with weak adhesions demonstrated a warpage phenomenon after only 30 min when it was heated on TEG. b) A RIG with intense adhesive properties exhibited a tightly attachment on the TEG surface after evaporative cooling of 12 h for the TEG. c–d) Corresponding COMSOL results of a,b). e) Schematics of results of evaporative cooling of RHG and RIG for working TEG in the motion, respectively. f) The temperature changes plotted with working time of engine, and the inset is an IR thermal image of engine after 1200 s. g) The acceleration of TEG when the engine was working. h) The results of evaporative cooling of RHG and RIG for TEG attached on a working engine, respectively, in which RIG could be firmly attached on TEG surface, but RHG was detached from the TEG. i) The electric outputs of the TEGs with RHG, RIG and without cooling system, respectively.

equipped with RIG when the heat source temperature is 50 °C. Moreover, the introduction of ionic liquid of [EMIM][Ac] enables the RIG strong adhesions with targeted substrates through diverse supramolecular forces. As a result, the TEG showed intense contacts with TEG surface both before and after hygroscopic processes, which ensured a stable evaporative cooling for TEG to durably boost its thermoelectric performance in both static and dynamic operation conditions. We believe that this type of hygroscopic ionogels with strong adhesions can provide a new avenue for heat dissipations designs for TEG to stably improve utilization and harvesting of waste heat in a sustainable and zero-carbon-footprint manner.

4. Experimental Section

Materials: Acrylic acid (AAc), 2-Acrylamido-2-methylpropane sulfonic acid (AMPSA), Ammonium persulfate (APS), and *N*, *N*-methylenebis (acrylamide) (MBAA) was obtained from Aladdin Shanghai Reagent Co., Ltd., and all chemicals were analytical grades and used as received.1-Ethyl-3-methylimidazolium acetate ([EMIM] [Ac]), 99% purity, was provided from Lanzhou Institute of Chemical Physics, Chinese Academy of Sciences. Graphene oxide (GO) slurry (7 wt% vs H_2O) was self-made through a modified Hummers method. The TEG was purchased from Changshan Wangu Electronic Technology Co., Ltd., China, which is consisted of two ceramic plates and 127-pairs of P–N type bismuth telluride sandwiched between them. The commercial Aluminum heat sink is consisted of aluminum alloy

6063, whose sizes were 25 × 25 × 5 mm and thermal conductivity of 201 W m^{-1} k^{-1}.

Fabrication of rGO Ionogels (RIG): The GO Slurry (0.5 g, 7 wt%) was dispersed in the 5 g [EMIM][Ac] via ultrasonication in an ice-bath for 1 h to acquire a homogeneous mixture (GO-[EMIM][Ac]). In this system, the ionogels are fabricated by a free radical polymerization. Typically, 1.8 g AAc, 0.3 g AMPSA, and 30 mg MBAA was added into resulted GO-[EMIM][Ac] to obtain a pregel solution. Next, the pregel solution was blowed with nitrogen for 10 min to remove oxygen, and then 0.1 g APS was added and mixed for initiation. Subsequently, the resulted solution was poured into a mould, and sealed for a thermal polymerization in an environment of 60 °C to obtain a piece of ionogel. Finally, the ionogels were put in a 90 °C oven for 2 days to reduce GO and remove residual water in ionogels to prepare the rGO ionogels (RIG). As a comparison, the rGO hydrogels (RHG) were fabricated similar methods by above, in which the [EMIM][Ac] was only replaced by DI water.

Materials Characterizations: The thermal stabilities of samples were measured by a TGA (TGA 8000-Spectrum two-Clarus SQ8T), in which the speed of temperature increasing was 5 °C min^{-1}. The functional groups of samples were measured by an ATR-FTIR. The emittances of materials were obtained from a Fourier Infrared Spectrometer (Nicolet 6700). The mechanical and adhesive properties of samples were tested by an Instron Universal Testing System (Instron, Z1.0). The rheological characterizations were performed on a Haake MARSIII rheometer equipped with a geometry of 25 mm parallel plates, where angular frequency ω was set from 0.1 to 100 rad s^{-1} at room temperature and under a fixed strain amplitude of 1%. Moreover, the dynamic temperature sweep was measured from the 25 to 120 °C at the rate of 2 °C min^{-1}, and the corresponding strain amplitude and angular frequency were 1% and 6.28 rad s^{-1}, respectively.

Moisture Sorption Experiments: The constant temperature and humidity testing machine (SANWOOD, SMC-80-CB-2) with high humidity uniformity (less than ± 1.5% RH) and high temperature uniformity (less than ± 0.5 °C) across the entire chamber was chosen to evaluate the moisture sorption performances of samples. The moisture sorption kinetics was measured at 25 °C and various RHs (50%, 70%, and 90%) for 12 h. The moisture sorption isotherms were assessed at 15, 25, and 35 °C, respectively. The moisture desorption was conducted in an oven, in which the desorption temperatures were designed as 60, 70, 80, and 90 °C, respectively. In the cyclic moisture sorption and desorption tests, the samples were put in an environment of 25 °C and 90% RH for 12 h, and then were took it into an oven of 90 °C for 12 h in every cycle. In these experiments, the initial sizes of samples were all cut into 10 × 10 × 5 mm. The mass change of the water sorption and desorption was recorded using an electronic scale (GXG, JJ224BC, 0.1 mg) at a regular interval. Additionally, the hygroscopic capacity of the RIG sample was calculated by

$$C_{RIG} = \Delta m / m_0 \tag{1}$$

where the C_{RIG} was the gravimetric moisture sorption capacity (g g^{-1}), the Δm referred to mass change before and after moisture sorption, and the m_0 is the weight of the whole dehydrated RIG.

Evaporative Cooling for Performance Promotion of TEG: The commercial TEG was used to harvest waste thermal energy and convert into electricity. In the systems, the low-grade waste heat was produced by a commercial heater, and corresponding heat source temperatures were set as 40, 50, 60, and 70 °C, respectively. Moreover, the RIG samples hydrated in different RH for 12 h were selected to dissipate heat from the TEG cold side through water evaporation. In these processes, corresponding mass changes of RIG samples and temperature varieties of TEG cold side were monitored by an electric scale and a multichannel temperature patrol instrument (JK 4008), respectively. The temperatures of RIG surface were captured using the IR thermal camera (Optris pi 400). In addition, the electric outputs were recorded by a multimeter to evaluate the evaporative-cooling capacity of resultant RIGs (Keithley 2100). All experiments were conducted in a constant environment of 25 °C and 50% RH. The original sizes of samples for evaporative-cooling experiments were designed as 20 × 20 × 5 mm. The practical area moisture sorption amount was defined as the mass change (Δm) per area of the dehydrated RIG.

Adhesive Testing of RIG: The adhesive forces between RIG and various adherends was characterized though 90° peeling-off and lap sheer measurements using a tensile testing machine (Instron, Z1.0). In these experiments, commercial TEG, glass, metal (Al), PET, and PTFE as adherends were selected.

In the 90° peeling-off testing, adherends were fixed on the testing machine, and 15 mm length of resulted RIG was prepeeled and clamped to the testing machine. Moreover, initial contact areas between RIG and adherends were all set as 30 × 10 mm. The peeling speed was constant in every measurement, which was set as 50 mm min^{-1}. Additionally, adhesive forces between RIG samples and adherends were determined by dividing the plateau force by the width of the RIG (10 mm).

In the lap sheer measurements, RIG samples (15 × 15 mm) were sandwiched between two pieces of adherends (45 × 15 mm). The adherends were clamped to the testing machine and the sheer speed was also set as 50 mm min^{-1}. The corresponding adhesive strengths were calculated by the maximum force by the contact area (15 × 15 mm).

In the cyclic adhesions of RIG, the tested RIG after peeling from the TEG was put in an oven of 90 °C for 1 h, and then was conducted the next peeling experiment.

The Dynamically Stable Evaporative Cooling of RIG on a Working Engine: Before evaporative cooling, the hydrated RIG sample was obtained from a dehydrated one with sizes were 20 × 20 × 5 mm through a 12 h moisture sorption in 90% RH. The resulted hydrated RIG and RHG were applied to dissipate heat from the cold side of the TEGs attached on working engine. The corresponding acceleration of TEG was measured by an acceleration sensor (HG 2506, HUIGE Instrument and METER Co., Ltd) and the temperature changes were monitored by IR thermal camera.

Supporting Information

Supporting Information is available from the Wiley Online Library or from the author.

Conflict of Interest

The authors declare no conflict of interest.

Data Availability Statement

Research data are not shared.

[1] G. Schierning, *Nat. Energy* **2018**, *3*, 92.

[2] A. Shakouri, *Annu. Rev. Mater. Res.* **2011**, *41*, 399.

[3] H. Cheng, J. Ouyang, *Adv. Energy Mater.* **2020**, *10*, 2001633.

[4] H. Cheng, X. He, Z. Fan, J. Ouyang, *Adv. Energy Mater.* **2019**, *9*, 1901085.

[5] Advanced Thermoelectric Materials for Energy Harvesting Applications, (Ed: S. Memon) IntechOpen, London 2019, Ch. 5.

[6] M. J. Deasy, N. Baudin, S. M. O'Shaughnessy, A. J. Robinson, *Appl. Energy* **2017**, *205*, 499.

[7] W. Ren, Y. Sun, D. Zhao, A. Aili, S. Zhang, C. Shi, J. Zhang, H. Geng, J. Zhang, L. Zhang, J. Xiao, R. Yang, *Sci. Adv.* **2021**, *7*, eabe0586.

[8] J. Liu, J. Zhang, J. Yuan, D. Zhang, J. Xing, Z. Zhou, *Sol. Energy Mater. Sol. Cells* **2021**, *220*, 110855.

[9] C. Wang, L. Hua, H. Yan, B. Li, Y. Tu, R. Wang, *Joule* **2020**, *4*, 435.

[10] H. Qi, T. Wei, W. Zhao, B. Zhu, G. Liu, P. Wang, Z. Lin, X. Wang, X. Li, X. Zhang, J. Zhu, *Adv. Mater.* **2019**, *31*, 1903378.

[11] F. Zhao, X. Y. Zhou, Y. Liu, Y. Shi, Y. F. Dai, G. Yu, *Adv. Mater.* **2019**, *31*, 1806446.

[12] X. Wang, X. Li, G. Liu, J. Li, X. Hu, N. Xu, W. Zhao, B. Zhu, J. Zhu, *Angew. Chem., Int. Ed.* **2019**, *58*, 12054.

[13] Y. Zhang, D. K. Nandakumar, S. C. Tan, *Joule* **2020**, *4*, 1.

[14] J. H. Humphrey, J. Brown, O. Cumming, B. Evans, G. Howard, R. N. Kulabako, J. Lamontagne, A. J. Pickering, E. N. Wang, *Lancet Planet. Health* **2020**, *4*, e91.

[15] X. Zhou, H. Lu, F. Zhao, G. Yu, *ACS Mater. Lett.* **2020**, *2*, 671.

[16] R. Li, Y. Shi, M. Wu, S. Hong, P. Wang, *Nat. Sustainable* **2020**, *3*, 636.

[17] S. Pu, J. Fu, Y. Liao, L. Ge, Y. Zhou, S. Zhang, S. Zhao, X. Liu, X. Hu, K. Liu, J. Chen, *Adv. Mater.* **2020**, *32*, 1907307.

[18] M. Wu, R. Li, Y. Shi, M. Altunkaya, S. Aleid, C. Zhang, W. Wang, P. Wang, *Mater. Horiz.* **2021**, *8*, 1518.

[19] W. Yu, G. Zhang, C. Liu, S. Fan, *ACS Nano* **2020**, *14*, 14091.

[20] H. Kim, S. Yang, S. R. Rao, S. Narayanan, E. A. Kapustin, H. Furukawa, A. S. Umans, O. M. Yaghi, E. N. Wang, *Science* **2017**, *356*, 430.

[21] N. Hanikel, M. S. Prevot, O. M. Yaghi, *Nat. Nanotechnol.* **2020**, *15*, 348.

[22] A. J. Rieth, A. M. Wright, G. Skorupskii, J. L. Mancuso, C. H. Hendon, M. Dinca, *J. Am. Chem. Soc.* **2019**, *141*, 13858.

[23] H. Kim, S. R. Rao, E. A. Kapustin, L. Zhao, S. Yang, O. M. Yaghi, E. N. Wang, *Nat. Commun.* **2018**, *9*, 1191.

[24] H. Yao, P. Zhang, Y. Huang, H. Cheng, C. Li, L. Qu, *Adv. Mater.* **2020**, *32*, 1905875.

[25] R. Li, Y. Shi, M. Alsaedi, M. C. Wu, L. Shi, P. Wang, *Environ. Sci. Technol.* **2018**, *52*, 11367.

[26] K. Yang, T. Pan, I. Pinnau, Z. Shi, Y. Han, *Nano Energy* **2020**, *78*, 105326.

[27] A. Karmakar, P. G. M. Mileo, I. Bok, S. B. Peh, J. Zhang, H. Yuan, G. Maurin, D. Zhao, *Angew. Chem., Int. Ed.* **2020**, *59*, 11003.

[28] F. Ni, N. Qiu, P. Xiao, C. Zhang, Y. Jian, Y. Liang, W. Xie, L. Yan, T. Chen, *Angew. Chem., Int. Ed.* **2020**, *59*, 19237.

[29] T. W. Gaines, M. H. Bell, E. B. Trigg, K. I. Winey, K. B. Wagener, *Macromol. Chem. Phys.* **2018**, *219*, 1700634.

[30] Y. Cao, Y. Chen, L. Lu, Z. Xue, T. Mu, *Ind. Eng. Chem. Res.* **2013**, *52*, 2073.

[31] A. J. Rieth, S. Yang, E. N. Wang, M. Dinca, *ACS Cent. Sci.* **2017**, *3*, 668.

[32] S. Yang, Y. Zhang, T. Wang, W. Sun, Z. Tong, *ACS Appl. Mater. Interfaces* **2020**, *12*, 46701.

[33] S. Pu, Y. Liao, K. Chen, J. Fu, S. Zhang, L. Ge, G. Conta, S. Bouzarif, T. Cheng, X. Hu, K. Liu, J. Chen, *Nano Lett.* **2020**, *20*, 3791.

[34] P. Yang, C. Feng, Y. Liu, T. Cheng, X. Yang, H. Liu, K. Liu, H. J. Fan, *Adv. Energy Mater.* **2020**, *10*, 2002898.

[35] J. W. Jeong, W. H. Yeo, A. Akhtar, J. J. Norton, Y. J. Kwack, S. Li, S. Y. Jung, Y. Su, W. Lee, J. Xia, H. Cheng, Y. Huang, W. S. Choi, T. Bretl, J. A. Rogers, *Adv. Mater.* **2013**, *25*, 6839.

[36] S. Wang, M. Li, J. Wu, D.-H. Kim, N. Lu, Y. Su, Z. Kang, Y. Huang, J. A. Rogers, *J. Appl. Mech.* **2012**, *79*, 031022.

[37] L. Pan, P. Cai, L. Mei, Y. Cheng, Y. Zeng, M. Wang, T. Wang, Y. Jiang, B. Ji, D. Li, X. Chen, *Adv. Mater.* **2020**, *32*, 2003723.

[38] J. Wei, Y. Zheng, T. Chen, *Mater. Horiz.* **2021**, https://doi.org/10.1039/D1MH00998B.

[39] Z. Yu, P. Wu, *Mater. Horiz.* **2021**, *8*, 2057.

[40] K. G. Cho, S. An, D. H. Cho, J. H. Kim, J. Nam, M. Kim, K. H. Lee, *Adv. Funct. Mater.* **2021**, *31*, 2102386.

[41] J. Zhu, X. Lu, W. Zhang, X. Liu, *Macromol. Rapid. Commun.* **2020**, *41*, 2000098.

[42] X. Shi, P. Wu, *Small* **2021**, *17*, 2101220.

[43] M. Gao, H. Wu, R. Plamthottam, Z. Xie, Y. Liu, J. Hu, S. Wu, L. Wu, X. He, Q. Pei, *Matter* **2021**, *4*, 1962.

[44] Z. Yu, P. Wu, *Adv. Mater.* **2021**, *33*, 2008479.

[45] G. Gao, F. Yang, F. Zhou, J. He, W. Lu, P. Xiao, H. Yan, C. Pan, T. Chen, Z. L. Wang, *Adv. Mater.* **2020**, *32*, 2004290.

[46] L. Zhang, K. S. Kumar, H. He, C. J. Cai, X. He, H. Gao, S. Yue, C. Li, R. C. Seet, H. Ren, J. Ouyang, *Nat. Commun.* **2020**, *11*, 4683.

[47] D. Gan, W. Xing, L. Jiang, J. Fang, C. Zhao, F. Ren, L. Fang, K. Wang, X. Lu, *Nat. Commun.* **2019**, *10*, 1487.

[48] S. Singla, G. Amarpuri, N. Dhopatkar, T. A. Blackledge, A. Dhinojwala, *Nat. Commun.* **2018**, *9*, 1890.

[49] D. Zhao, Y. Zhu, W. Cheng, G. Xu, Q. Wang, S. Liu, J. Li, C. Chen, H. Yu, L. Hu, *Matter* **2020**, *2*, 390.

[50] Y. Xu, R. Rothe, D. Voigt, S. Hauser, M. Cui, T. Miyagawa, M. Patino Gaillez, T. Kurth, M. Bornhauser, J. Pietzsch, Y. Zhang, *Nat. Commun.* **2021**, *12*, 2407.